The Astrophysical Journal, 636:L153–L156, 2006 January 10

NEAR-INFRARED IMAGES OF PROTOPLANETARY DISK SURROUNDING HD 142527[1]

Misato Fukagawa,[2,3] Motohide Tamura,[4,5] Yoichi Itoh,[6] Tomoyuki Kudo,[5] Yusuke Imaeda,[6] Yumiko Oasa,[6] Saeko S. Hayashi,[5,7] and Masahiko Hayashi[5,7]

Received 2005 August 28; accepted 2005 November 30; published 2006 January 3

ABSTRACT

We discovered a unique morphology in a disk around the Herbig Ae star HD 142527 by near-infrared (*H* and *K* bands) adaptive optics imaging observations. The almost face-on disk consists of two bright arcs facing one another along the east-west direction (banana-split structure) and one spiral arm extending to the north from the western arc. The eastern arc is located at ∼100–400 AU in radius from the star, and the western one is detected at ∼150–490 AU. The stellar position is displaced from the center of the disk by about 20 AU to the north, and also from the center of the inner hole. The two arcs show an asymmetry in their size and brightness; the larger western arc is brighter than the east one by about 2 mag. The morphology of the disk, consisting of a banana-split structure and a spiral arm, most likely suggests the presence of an unseen eccentric binary and a recent stellar encounter.

Subject headings: stars: pre–main-sequence — planetary systems: protoplanetary disks — stars: individual (HD 142527)

1. INTRODUCTION

Circumstellar disks are ubiquitous around low- to intermediate-mass ($M_* \lesssim 5\ M_\odot$) pre–main-sequence (PMS) stars with excess infrared emission. Their existence and properties have been established on the basis of observed spectral energy distributions (SEDs). However, knowledge of their morphology is indispensable to a better understanding of disk formation and evolution. Recent images of outer disks with a resolution of $\lesssim 0''.1$ obtained using space- and ground-based telescopes revealed various detailed spatial structures of disks, and these structures are hard to predict from SEDs (Fukagawa et al. 2004). The morphological variety may result from the fact that the disk property depends on a combination of parameters such as stellar age, multiplicity, and initial disk mass. As a new example of disk morphology, in this Letter we present the near-infrared (NIR) images of a disk around HD 142527.

HD 142527 (F6 IIIe) is classified as a Herbig Ae star, as confirmed by its spectra and photometry, which exhibit the typical characteristics of a PMS star (Waelkens et al. 1996). The *Hipparcos* measurements suggest that its distance is 200 pc, but with a large uncertainty in parallax of over 20%. Since HD 142527 ($l = 335^\circ.7$, $b = 8^\circ.5$) is a probable member of Lupus (Upper Centaurus Lupus; de Zeeuw et al. 1999; Teixeira et al. 2000), we adopt the mean distance of that moving group, $d = 140$ pc, as the distance to HD 142527. The stellar age and mass are 2^{+2}_{-1} Myr and $1.9 \pm 0.3\ M_\odot$, respectively, estimated from its stellar luminosity in the UV and optical wavelengths and from the isochrone of Palla & Stahler (1999).

The uniqueness in its SED has been recognized; its infrared excess is larger than the stellar luminosity, which is difficult to reconcile with a simple reprocessing disk, even though there is no strong rise in the mid-infrared (MIR) SED like those often seen in young stars with active accretion (Dominik et al. 2003). HD 142527 has also been identified by the resemblance of its infrared spectra to those seen in solar comets and by the highest crystallinity of circumstellar dust among other Herbig Ae disks with similar or older ages (van Boekel et al. 2004).

The unique SED and dust processing timescale may be due to unique density and temperature distributions in the disk that should be reflected in the morphology. In addition, the disk structure and its evolution might depend on such environmental effects as companion stars. Resolving the circumstellar environment may thus provide an important insight into the nature of the protoplanetary disk around HD 142527. For this purpose, we conducted the adaptive optics (AO) imaging of HD 142527 with a spatial resolution of $0''.13$, using the coronagraphic camera CIAO (Coronagraphic Imager with Adaptive Optics; Tamura et al. 2000) on the Subaru Telescope.

2. OBSERVATIONS AND DATA REDUCTION

We carried out coronagraphic imaging observations of HD 142527 in the *H* and *K* bands on 2004 June 5 and 6, respectively. CIAO utilizes the 1024 × 1024 InSb ALADDIN II array at the second focal plane. The pixel scale was 21.3 mas pixel^{-1}. We used the coronagraph, a combination of a circular occulting mask at the first focal plane and a circular Lyot stop at the pupil plane, to block out the outer 20% of the pupil diameter. The coronagraphic mask has a transmission of 1%–2%, which allows us to measure the position of an occulted star and to detect a companion star even inside the mask if it exists.

For the *H*-band imaging, we used the occulting mask with a diameter of $1''.0$. The spatial resolution (FWHM) of $0''.13$ was achieved by using the AO under the natural seeing of $0''.5$ (at optical) at the time of this observation. The exposure time was 5 s for each data frame, and 272 frames were taken in total. Because the obtained images suffered from seeing variation, 92 frames were combined to produce the disk image after unusable frames were rejected, as described later. As point-spread function (PSF) reference stars, we observed HD 137785 and HD 145191 before and after HD 142527, respectively. Both stars are located within 10° from HD 142527. They have the same *R* magnitudes as that of HD 142527 after their fluxes were attenuated with the

[1] Based on data collected at the Subaru Telescope, which is operated by the National Astronomical Observatory of Japan.

[2] *Spitzer* Science Center, California Institute of Technology, Mail Code 220-6, Pasadena, CA 91125; misato@ipac.caltech.edu.

[3] Nagoya University, Furo-cho, Chikusa-ku, Nagoya 464-8602, Japan.

[4] National Astronomical Observatory of Japan, 2-21-1 Osawa, Mitaka, Tokyo 181-8588, Japan.

[5] Department of Astronomical Science, The Graduate University for Advanced Studies (SOKENDAI), 2-21-1 Osawa, Mitaka, Tokyo 181-8588, Japan.

[6] Graduate School of Science and Technology, Kobe University, 1-1 Rokkodai, Nada, Kobe 657-8501, Japan.

[7] Subaru Telescope, National Astronomical Observatory of Japan, 650 North A'ohoku Place, Hilo, HI 96720.

neutral density filters for the AO (both HD 142527 and reference stars were too bright for the AO) to obtain similar PSFs as that of HD 142527. The total exposure time was 660 s for each reference star. The *K*-band images were obtained with a smaller mask of 0″.6 diameter in addition to the images with a 1″.0 one, in order to confirm the inner hole that we detected in the *H*-band images taken on the night before. For the 1″.0 mask images, the exposure time was 3 s, and two exposures were co-added into one frame. The seeing condition was worse, and we chose 27 frames to produce the final image among the obtained 110 frames. For the 0″.6 mask images, six exposures of 1 s were co-added into one frame, and a total of 60 frames was taken. In order to obtain the same spatial resolution as that of the *H* band, only seven frames were usable. It was, however, sufficient to confirm the existence of the inner hole. In the same manner as for the *H*-band imaging, we observed HD 137785 and HD 145191 as PSF reference stars. The total exposure time of PSF stars was 240 and 840 s for 1″.0 and 0″.6 mask imaging, respectively.

The obtained images were first processed using the IRAF packages for dark subtraction, flat-fielding with sky flats, bad pixel correction, and sky subtraction. Although the existence of circumstellar structure was obvious even in the unreduced images, PSF subtraction was required to investigate the structure buried in the halo of the central bright star. First, we excluded the frames in which the PSFs had larger sizes than others for the data set of HD 142527. The PSF size was evaluated based on the brightness ratio between the peak and the halo at $r = 1''.5$. Second, in the same manner, appropriate frames were adopted for the PSF reference images, in order for the stellar PSF sizes to be similar to those of HD 142527. Because of the very bright structure around HD 142527, the brightness ratio between peak and halo was not valid as a quantitative measure for matching PSFs between HD 142527 and the reference stars. We therefore checked the results of the PSF subtraction to see whether or not the stellar halo was subtracted sufficiently, selecting the acceptable PSF size as the reference PSF. After careful selection, the reference PSF was made by combining the adopted reference star images. The PSF was shifted to match the position of the occulted star, rotated to match the direction of the spider pattern, and subtracted from each data frame of HD 142527. The flux scaling of the PSF was performed so that no region had negative intensity after the subtraction, in particular, just outside the mask (the inner hole). Although this scaling method gave the lower limit to the disk brightness, the brightness uncertainty was within 15% in order to subtract the circular halo of the star. After the frames with mismatched PSF shapes were excluded, 92 PSF-subtracted frames (460 s integration) were combined for the *H* band, 27 frames (162 s) for the *K* band with the 1″.0 mask, and seven frames (42 s) for the *K* band with the 0″.6 mask.

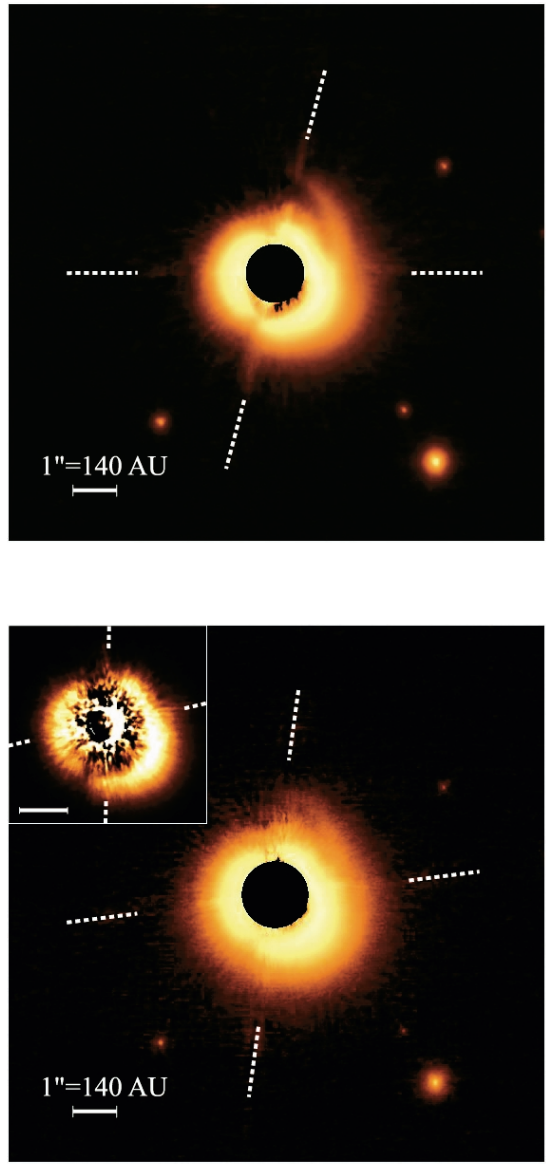

FIG. 1.—*H*- (*top*) and *K*-band (*bottom*) images of the disk around HD 142527. The central software mask has a radius of $r = 0''.66$ (*top*) and $r = 0''.75$ (*bottom*). The images are displayed in logarithmic scale. In the upper left-hand corner of the bottom panel, the image taken with the smaller occulting mask (0″.6 in diameter) is presented in order to show that the inner hole extended to the southwest is not an artifact. The image is linearly scaled. In all images, the white dotted lines indicate the secondary spider directions. North is up, and east is to the left.

3. RESULTS

The bright circumstellar structure was detected in both *H* and *K* bands with very similar appearances, as is shown in Figure 1. In the deeper *H*-band images, the scattered light was detected out to the radius $r = 3''.5$ where the brightness drops to the 1 σ level in the most extended southwest direction along P.A. ∼ 240°. At a distance $d = 140$ pc of HD 142527, the outer radius corresponds to 490 AU, which is the typical size for the protoplanetary disks observed so far.

Of particular interest is the disk morphology shown by our images. Basically, the disk resembles a ring with an inner hole. The inner hole is a real structure, not an artifact caused by the PSF subtraction. This has been confirmed by observations at the two wave bands *H* and *K* and with a smaller mask imaging in the *K*. The stellar position and the center of the hole differ noticeably; the edge of the hole is located at $r \sim 100$ AU on the east side of the star, and $r \sim 150$ AU on the west side when measured along P.A. = 60°. The displacement is also significant when we compare the stellar position with the center of the disk defined by the center of a fitted ellipse. The star is located ∼0″.16 (=20 AU) north from the center of the ellipse with P.A. = 60°. Taking a closer look at the ring in Figure 2, we see that the circular emission is not continuous. The brightness distribution is better represented by two elliptical arcs facing one another rather than a ring with northern and southern gaps. In addition, a spiral arm is observed, extending to the north from the western arc. No counterarm is detected.

A strong brightness asymmetry exists between the south-

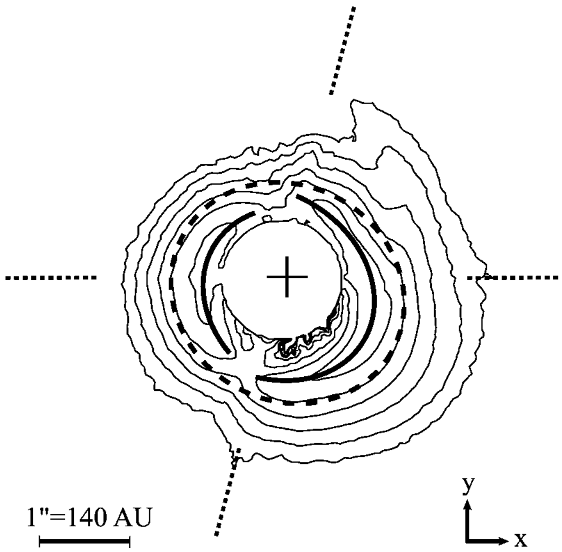

FIG. 2.—*H*-band contours, indicated in the range of 11–15 mag arcsec^{-2} with each interval of 0.8 mag arcsec^{-2}. The plus sign corresponds to the position of the visible star. The dashed ellipse has an axis ratio of 0.1, and its central position $(\Delta x, \Delta y) = (0, -23)$ AU from the star. The bold arcs show parts of ellipses with their eccentricity of 0.2, and their central positions of $(\Delta x, \Delta y) = (+42, -42)$ AU and $(\Delta x, \Delta y) = (-42, -6)$ AU for the eastern and western components, respectively.

western and northeastern parts, as seen in the radial surface brightness profile (Fig. 3). The southwestern side is brighter than the northeastern side by about 2 mag in the direction of P.A. = 240°. The anisotropic scattering could contribute to this brightness asymmetry, as dust grains scatter the incident light in a forward direction. In the optical images of the Digitized Sky Survey, a faint nebulosity can be found, and the southwest region is brighter as well. This suggests that the disk around HD 142527 is likely inclined, as the southwestern side is nearer to us, assuming that the nebular material is distributed uniformly. On the other hand, if the disk has a circular shape, without being affected by additional gravitational sources as described later, its ellipticity of around 0.15 (see Fig. 2) implies that the disk is slightly inclined ($i \sim 30°$) along the northwest-southeast direction. In this case, the observed brightness asymmetry cannot be attributed to anisotropic scattering but rather is attributed to the different amount of scatterers.

The outer edges of the east and west arcs are sharp compared with the outer regions of the other resolved disks. In particular, the surface brightness of the northeastern side decreases more steeply than that of the southwest side. The fitting of a power-law function gives the radial profiles in the *H* band as $r^{-6.6\pm0.1}$ ($1\farcs5 \le r \le 2\farcs6$) and $r^{-8.9\pm0.1}$ ($1\farcs3 \le r \le 1\farcs8$) for the southwest and northeast sides, respectively. Note that the radial profile for the western disk represents the combined effect of the arc and the spiral arm, especially inside $2\farcs5$ in radius. Although the structure in the *K* band is slightly blurred compared with that in the *H* band, the $H-K$ color does not significantly change in azimuthal direction. The color of the scattered light is almost the same as the color of the total flux, including the stellar and thermal emission from the inner dust disk ($H-K = 0.74$; Malfait et al. 1998). The same color is also confirmed by the ratio of scattered light to total flux. We calculated the scattered flux, $F_{\rm scatt}$, by integrating the surface brightness in the radial range of $0\farcs75 \le r \le 3\farcs0$, and we obtained $F_{\rm scatt} = 130 \pm 9$ mJy and $F_{\rm scatt} = 170 \pm 10$ mJy in the *H* and *K* bands, respectively. Taking the total flux ($F_{\rm tot}$) from the literature (Malfait et al. 1998), we obtained $F_{\rm scatt}/F_{\rm tot} = (3.1 \pm 0.2) \times 10^{-2}$ in the *H* band and $(3.2 \pm 0.2) \times 10^{-2}$ in the *K* band. This can be interpreted as gray scattering, assuming that the scattered light originates from dust grains at the same height above the disk midplane at both wavelengths. The gray scattering suggests that the size of the grains responsible for the scattering is $\gtrsim 1$ μm, which is larger than the grains in the interstellar medium.

4. DISCUSSION

The resolved images revealed unique features: facing arcs with a large inner hole, stellar displacement, a steep outer edge, and one spiral arm. The hole was not predicted as there was no obvious dip in the MIR SED. A rough estimate suggests that the inner edge, at $R_{\rm in} = 150$ AU, emits the most at 50 μm, assuming $R_{\rm in}T_{\rm in}^2 = R_* T_*^2$ inside the observed disk, and using $\log T_* = 3.78$ and $R_* = 2.9\ R_\odot$, as deduced by the SED fitting. Other MIR emitters, such as an unseen companion star, might be required to compensate for the missing flux in MIR. Note that our observations cannot distinguish an inner disk, if any, inside the occulting mask ($r \lesssim 0\farcs5 = 70$ AU). Since the large NIR excess flux, MIR silicate features (van Boekel et al. 2004), and spatially resolved 10 μm emission (Leinert et al. 2004) suggest the dust distribution in the vicinity of a star, the hole is likely to be a gap separating the inner and outer disks. The stellar displacement from the center of the disk is usually seen for the

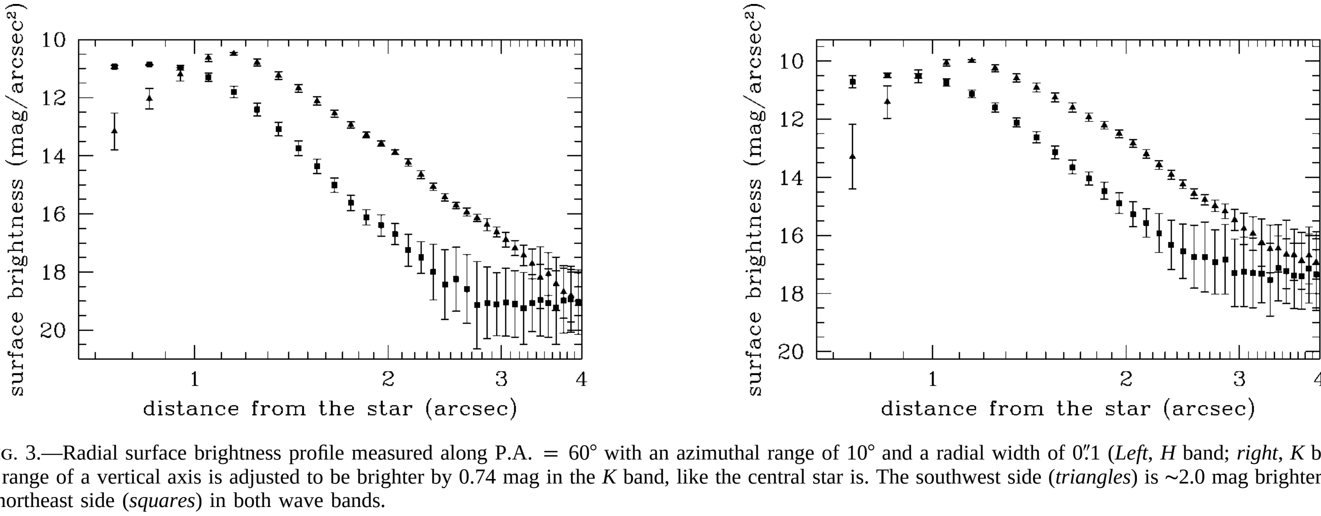

FIG. 3.—Radial surface brightness profile measured along P.A. = 60° with an azimuthal range of 10° and a radial width of $0\farcs1$ (*Left*, *H* band; *right*, *K* band). The range of a vertical axis is adjusted to be brighter by 0.74 mag in the *K* band, like the central star is. The southwest side (*triangles*) is ~2.0 mag brighter than the northeast side (*squares*) in both wave bands.

flared disk if it is along the minor axis of the projected disk (Vinković et al. 2003). The off-center of HD 142527 could be also due to the flaring if the disk is inclined along the northwest-southeast direction. On the other hand, assuming that the disk is inclined so that the southwest is the near side, the displacement is a real feature. We cannot discriminate both possibilities at present, but in any case, the displacement from the center of the inner hole along roughly the major axis is remarkable.

The observed disk morphology implies dynamical effects on dust particles distributed around HD 142527. A morphology similar to the facing arcs is found in the numerical simulations by Adams et al. (1989), in which the alternating arcs, called the "banana-split" regime in their paper, were a result of the extreme case of one-armed dynamical instability. However, such eccentric instability is ineffective unless the disk is heavier than the central star (e.g., Taga & Iye 1998). The disk mass of HD 142527 is estimated to be 0.15 $M_\odot$ (Acke et al. 2004), which is relatively massive for a disk of one million years of age but is still too small to induce this instability. Therefore, it is unlikely that this instability would account for the observed banana-split structure.

In contrast, an eccentric disk forms by a central binary system, even for a less massive disk, if the binary eccentricity is $e_B \geq 0.2$ (Nelson 2003), a value that is within the majority of the known spectroscopic binaries (Duquennoy & Mayor 1991; Mathieu 1994). If the disk eccentricity is driven by a central binary in a steady orbital motion, the eccentric disk is expected to be long-lived and highly observable. Observationally, however, no firm evidence has been obtained for the binarity of HD 142527, except for the speculation of a red companion in order to explain the large infrared excess (Leinert et al. 2004). The interaction of a central binary with a disk leads to the truncation of the inner edge of the circumbinary disk. The size of its inner radius depends on the mass ratio q and the eccentricity e_B. For instance, the radius of the hole is around 3a–4a for $q \lesssim 0.5$ and $e_B \sim 0.5$, where a is the binary semimajor axis (Artymowicz & Lubow 1994). Considering an inner edge of ~150 AU, an invisible companion could lie inside the masked region ($r \lesssim 0''.5 = 70$ AU) and should have been detected with an imaging resolution of $0''.1$ ($=14$ AU) if bright enough. Our deep H-band image constrains the mass of the putative companion star. In the masked region, which is not completely opaque, a point source with $H < 9.0$ mag could be detected. Given the age and the distance, we expect a companion star of, at most, 0.5 $M_\odot$ if its infrared excess is insufficient (Palla & Stahler 1999). This gives an upper limit to the mass ratio of $q < 0.25$. The stellar displacement from the center of the hole suggests that a low-mass companion, if any, is located relatively far from the star. Therefore, the possibility of a larger mass companion closer to the star can be excluded.

We should note that there is a discrepancy between the calculations and observations. The prediction based on a simplified disk model shows that only one arc is expected and that two may have difficulty emerging under reasonable physical conditions (Imaeda 2005). Since the disk shows an additional spiral arm that cannot be simultaneously reproduced in an eccentric disk, the actual system appears to be more complicated than the simple model consisting only of a central binary and a circumbinary disk. However, the inner hole still implies the presence of a central binary, as it is the most robust cause of the hole in a PMS disk. We also cannot rule out Jupiter-mass planet(s) opening the hole along its orbit, although it would be difficult for such a small-mass perturber to form the banana-split morphology over the disk. The limiting magnitude of $H = 15.3$ mag in the southern part of the hole ($r \sim 0''.8$) gives the mass upper limit of an undetected planet, $\sim 10 M_J$ (Baraffe et al. 2003). The gap is too wide (>80 AU in the southern region) and azimuthally asymmetric for that opened by a Jupiter-mass planet in a circular orbit, but it might be accounted for by an eccentric planet.

The spiral arm in the western arc is suggestive of a recent stellar encounter (Larwood & Kalas 2001; Quillen et al. 2005). In the simulation studies (Pfalzner 2003), the asymmetric spiral arms are produced with one strong arm due to interaction with a passing star and a counterarm due to stellar displacement from the center of the mass of the system. The central disk structure may also be affected by the flyby, giving the elliptical shape. The stars passing close to HD 142527 could belong to the same moving group; thus, they may have ages and distances similar to those of HD 142527. In our observations of the 20″ field of view, several sources were detected around HD 142527. The fluxes of three point sources were measured within 0.2 mag uncertainties, but they are faint ($14.5 \text{ mag} < K < 17$ mag) and do not show red colors as an indicator of youth ($H - K < 0.2$), suggesting that they could be background stars. Since the arm structure is transient but is thought to be sustained for $\sim 10^3$ yr, the perturber may exist outside our field of view, considering the mean proper motion of the Lupus moving group [$(\mu_\ell \cos b,\ \mu_b) = (-30.1 \pm 0.1, -9.1 \pm 0.1)$ mas yr^{-1}; de Zeeuw et al. 1999]. Follow-up observations to identify perturbers inside and outside of the disk should improve our understanding of this system and the effects of perturbers on protoplanetary disks.

We appreciate the support from the Subaru Telescope staff. We are grateful to Shigeru Ida for valuable discussions. M. F. is supported by the JSPS Research Fellowships for Young Scientists. This work was partially supported by the Grants-in-Aid for Scientific Research (16740256 and 16077204) of the MEXT.

REFERENCES

Acke, B., van den Ancker, M. E., Dullemond, C. P., van Boekel, R., & Waters, L. B. F. M. 2004, A&A, 422, 621
Adams, F. C., Ruden, S. P., & Shu, F. H. 1989, ApJ, 347, 959
Artymowicz, P., & Lubow, S. H. 1994, ApJ, 421, 651
Baraffe, I., Chabrier, G., Barman, T. S., Allard, F., & Hauschildt, P. H. 2003, A&A, 402, 701
de Zeeuw, P. T., Hoogerwerf, R., de Bruijne, J. H. J., Brown, A. G. A., & Blaauw, A. 1999, AJ, 117, 354
Dominik, C., Dullemond, P., Waters, L. B. F. M., & Walch, S. 2003, A&A, 398, 607
Duquennoy, A., & Mayor, M. 1991, A&A, 248, 485
Fukagawa, M., et al. 2004, ApJ, 605, L53
Imaeda, Y. 2005, in Protostars and Planets V, ed. V. Mannings et al. (LPI Contribution No. 1286; Houston: LPI), 8305
Larwood, J. D., & Kalas, P. G. 2001, MNRAS, 323, 402
Leinert, Ch., et al. 2004, A&A, 423, 537
Malfait, K., Bogaert, E., & Waelkens, C. 1998, A&A, 331, 211
Mathieu, R. D. 1994, ARA&A, 32, 465
Nelson, R. P. 2003, MNRAS, 345, 233
Palla, F., & Stahler, S. W. 1999, ApJ, 525, 772
Pfalzner, S. 2003, ApJ, 592, 986
Quillen, A. C., Varnière, P., Minchev, I., & Frank, A. 2005, AJ, 129, 2481
Taga, M., & Iye, M. 1998, MNRAS, 299, 1132
Tamura, M., et al. 2000, Proc. SPIE, 4008, 1153
Teixeira, R., Ducourant, D., Sartori, M. J., Camargo, J. I. B., Périé, J. P., Lépine, J. R. D., & Benevides-Soares, P. 2000, A&A, 361, 1143
van Boekel, R., et al. 2004, Nature, 432, 479
Vinković, D., Ivezić, Ž., Miroshnichenko, A. S., & Elitzur, M. 2003, MNRAS, 346, 1151
Waelkens, C., et al. 1996, A&A, 315, L245